Arch Obstet Gynecol. 2026;7(1):35–48.

Archives of Obstetrics and Gynaecology Original Research

Evaluation of Adenomyosis by MUSA Based Transvaginal Ultrasound in Women Undergoing Hysterectomy

Merve Nur Taşpınar[1], Çetin Çelik[1], Ersin Çintesun[1,*]

[1]Department of Obstetrics and Gynecology, Selçuk University Faculty of Medicine, Konya, Turkey

[*]Correspondence should be addressed to Ersin Çintesun, ersincintesun@gmail.com

Received date: July 06, 2026, **Accepted date:** July 14, 2026

Citation: Taşpınar MN, Çelik C, Çintesun E. Evaluation of Adenomyosis by MUSA Based Transvaginal Ultrasound in Women Undergoing Hysterectomy. Arch Obstet Gynecol. 2026;7(1):35–48.

Abstract

Introduction: Adenomyosis diagnosis has improved substantially with high-resolution transvaginal ultrasound and the standardized Morphological Uterus Sonographic Assessment (MUSA) criteria; however, the relative diagnostic contribution of individual sonographic signs to histopathological confirmation remains incompletely defined. This study evaluated clinical and ultrasonographic markers associated with histopathologically confirmed adenomyosis.

Materials and methods: We conducted a single-center prospective observational study of consecutive women scheduled for hysterectomy at a tertiary referral center. Clinical symptoms and a comprehensive set of direct and indirect MUSA criteria were systematically recorded using a standardized reporting form. Associations with histopathologically confirmed adenomyosis were evaluated by univariate logistic regression; Odds Ratios (OR) with 95% Confidence Intervals (CI) and corresponding p-values are reported. A multivariable model was not constructed owing to sample size constraints and the exploratory nature of the study.

Results: Clinically, Heavy Menstrual Bleeding (HMB) demonstrated the strongest association with adenomyosis (OR=4.81, 95% CI: 2.33–9.92; p<0.001), followed by dyspareunia (OR=1.11, 95% CI: 1.01–1.23; p=0.02). Dysmenorrhea, chronic pelvic pain, dyschezia, and dysuria were not statistically significant predictors in univariate analysis. Ultrasonographically, five MUSA criteria demonstrated statistically significant associations with histopathologically confirmed adenomyosis: subendometrial echogenic lines/buds (OR=8.51, 95% CI: 2.20–32.9; p<0.001), myometrial asymmetry (OR=6.88, 95% CI: 2.22–21.3; p<0.001), myometrial heterogeneity (OR=4.96, 95% CI: 1.28–19.3; p=0.015), myometrial cysts (OR=3.30, 95% CI: 1.67–6.56; p<0.001), and junctional zone irregularity (OR=2.57, 95% CI: 1.18–5.40; p=0.047). In contrast, uterine size in the leiomyoma-free subset, myometrial shadowing patterns, lesion vascularization, lesion echogenicity, and lesion definition demonstrated no statistically significant associations with adenomyosis. Hyperechoic islands showed a non-significant trend toward association with adenomyosis (OR=2.67, 95% CI: 0.94–7.52; p=0.058). Myometrial cysts demonstrated a sensitivity of 67.3% and specificity of 61.6%; subendometrial echogenic lines/buds showed lower sensitivity (17.3%) but higher specificity (97.6%) for histopathologically confirmed adenomyosis.

Conclusion: Transvaginal ultrasound incorporating MUSA criteria is clinically useful for preoperative adenomyosis diagnosis, particularly through markers like subendometrial lines, myometrial asymmetry, heterogeneity, cysts, and junctional zone irregularity.

Keywords: Adenomyosis, Transvaginal ultrasound, MUSA criteria, Myometrial cysts, Subendometrial echogenic lines, Junctional zone, Heavy menstrual bleeding, Dyspareunia, Hysterectomy

Introduction

Adenomyosis is a chronic, estrogen- and progesterone-dependent benign uterine condition defined by the ectopic presence of endometrial glands and stroma within the myometrium, accompanied by adjacent smooth muscle hyperplasia and hypertrophy. It is increasingly recognized as a heterogeneous condition with distinct subtype's inner, outer, and diffuse myometrial involvement each potentially differing in pathogenesis, clinical presentation, and treatment response [1]. The clinical spectrum ranges from incidental asymptomatic findings to severe dysmenorrhea, heavy menstrual bleeding, chronic pelvic pain, dyspareunia, and infertility, with significant impairment of health-related quality of life [2].

The true prevalence of adenomyosis remains uncertain. Histopathological examination of hysterectomy specimens has reported widely varying rates of 5–70%, with a consensus estimate of approximately 20–35% when standardized diagnostic criteria are applied [3]. However, with the advent of high-resolution transvaginal ultrasound and improved imaging protocols, adenomyosis is increasingly identified in younger, nulliparous, and infertile women who would not previously have been captured in hysterectomy-based prevalence studies, suggesting that the true population prevalence may be substantially higher than historically reported [4,5].

The pathogenesis of adenomyosis remains incompletely understood. The most widely accepted hypothesis involves invagination of the endometrial basalis layer into the inner myometrium along the junctional zone, facilitated by tissue injury and repair (TIAR) mechanisms, which are thought to be triggered by uterine peristaltic dysfunction, repeated microtraumatic insults, and altered immune surveillance [1,6]. Alternative pathogenic hypotheses include de novo development from Müllerian remnants, metaplasia of adult stem cells, and lymphatic or hematogenous dissemination of endometrial cells [6]. Regardless of the initiating mechanism, ectopic endometrial tissue within the myometrium induces a sustained localized inflammatory response, smooth muscle hyperplasia and hypertrophy, aberrant angiogenesis, and progesterone resistance — collectively contributing to the hallmark clinical manifestations of heavy menstrual bleeding and pelvic pain [1].

The Morphological Uterus Sonographic Assessment (MUSA) consensus was first published in 2015, establishing standardized terminology and sonographic criteria for uterine morphological evaluation [7]. In 2022, a modified Delphi procedure led to a substantive revision of MUSA definitions, refining the classification of direct adenomyosis markers — including myometrial cysts, hyperechoic islands, and subendometrial echogenic lines and buds — and indirect markers, comprising myometrial asymmetry, myometrial heterogeneity, junctional zone irregularity, fan-shaped shadowing, and translesional vascularization [8]. These updated 2022 MUSA criteria form the methodological backbone of the present study and represent the current standard for sonographic adenomyosis assessment in both clinical practice and research settings. The concurrent presence of multiple sonographic markers has been shown to improve overall diagnostic accuracy, and MUSA criteria additionally facilitate differentiation between focal and diffuse adenomyosis subtypes, thereby informing individualized clinical management decisions [7–9].

Accurate preoperative identification of adenomyosis in patients scheduled for hysterectomy is important for patient counseling and for objective assessment of surgical indications [10]. Evaluating the concordance between preoperative transvaginal ultrasound using MUSA criteria and postoperative histopathological diagnosis will help determine the clinical utility of these sonographic criteria.

While magnetic resonance imaging (MRI) is considered the reference standard for adenomyosis diagnosis with reported sensitivity of 77–78% and specificity of 85–89%, its limited availability, higher cost, and patient-related contraindications restrict its routine clinical use. Transvaginal ultrasound, particularly when performed using standardized MUSA criteria by trained operators, achieves comparable diagnostic performance and remains the first-line imaging modality recommended by international guidelines including ESHRE and ISUOG [10,11].

The primary aim of this study was to evaluate the association between preoperative transvaginal ultrasound findings based on MUSA criteria and histopathologically confirmed adenomyosis in women undergoing hysterectomy at a tertiary referral center. Secondary aims included: (i) assessment of the individual diagnostic value of direct and indirect MUSA sonographic markers; (ii) identification of clinical symptoms independently associated with adenomyosis in univariate analysis; (iii) estimation of odds ratios with 95% confidence intervals for each clinical and sonographic marker to quantify the magnitude of association with adenomyosis; and (iv) evaluation of the additive diagnostic value of a composite MUSA score derived from eight binary sonographic criteria.

Materials and Methods

Study design and ethical approval

This prospective observational cohort study was conducted at a single tertiary referral center (Department of Obstetrics and Gynecology, Selçuk University Faculty of Medicine, Konya, Turkey) between December 2024 and January 2026. The study was designed, conducted, and reported in accordance with the Strengthening the Reporting of Observational Studies in Epidemiology (STROBE) guidelines for prospective observational cohort studies. Ethical approval was obtained from the Selçuk University Faculty of Medicine Clinical Research Ethics Committee (Registration No: E.892571; Decision No: 2024/22). The study was conducted in accordance with the principles of the Declaration of Helsinki (2013 revision) and applicable Good Clinical Practice guidelines. Written informed consent was obtained from all participants prior to enrollment. A total of 177 women were included in the final analysis. A priori power analysis was performed based on an expected adenomyosis prevalence of 25–30% in the hysterectomy population, a minimum detectable odds ratio of 2.5 for key sonographic markers, 80% statistical power, and a two-sided

alpha level of 0.05, indicating a required minimum sample size of approximately 150 participants. The final enrolled sample of 177 women was therefore considered adequate to meet the primary study objectives. However, given the exploratory nature of the study and the absence of multivariable modeling, findings should be interpreted with appropriate caution.

Inclusion and exclusion criteria

Inclusion criteria were (i) Women aged 18–52 years; (ii) scheduled for hysterectomy for benign or malignant gynecological indications; and (iii) provision of written informed consent prior to enrollment. Exclusion criteria were (i) incomplete clinical or ultrasonographic data precluding full MUSA assessment; (ii) prior uterine surgery including myomectomy, endometrial ablation, or cesarean section, owing to potential distortion of myometrial architecture and junctional zone morphology; (iii) current pregnancy or postpartum state within six months of examination; (iv) inadequate or insufficient histopathological specimens precluding definitive adenomyosis assessment; (v) use of hormonal therapy within three months prior to ultrasound examination, including combined oral contraceptives, progestins, GnRH analogues, or levonorgestrel-releasing intrauterine system, due to potential suppression of sonographic adenomyosis features; (vi) known or suspected uterine or endometrial malignancy at the time of ultrasound examination; and (vii) technically inadequate transvaginal ultrasound examination due to patient body habitus or probe intolerance.

Clinical data collection

Demographic and clinical data, surgical indications, and preoperative endometrial pathology results were prospectively recorded on a standardized data collection form. Histopathological diagnosis of adenomyosis was based on internationally accepted standardized criteria: the presence of endometrial glands and stroma within the myometrium, located more than 2.5 mm (one low-power microscopic field) below the endometrial-myometrial junction, accompanied by adjacent smooth muscle hyperplasia and hypertrophy [12]. All hysterectomy specimens were evaluated by a single experienced gynecological pathologist who was blinded to preoperative ultrasound findings and clinical symptom data. Tissue sections were obtained at standardized intervals of 3–5 mm throughout the full thickness of the uterine wall to minimize sampling error and ensure adequate histopathological representation [12]. All women were systematically questioned about the presence and severity of chronic pelvic pain, abdominal bloating, dysmenorrhea, dyspareunia, dysuria, and dyschezia during a structured preoperative interview. Symptom severity was quantified using a validated 10-point Visual Analog Scale (VAS), where 0 indicated complete absence of symptoms and 10 indicated the worst imaginable pain intensity. VAS assessments were conducted exclusively by a single trained investigator to minimize interobserver variability. Symptoms were recorded as present if the VAS score was ≥1. VAS scores were additionally analyzed as continuous variables to preserve full distributional information. Heavy menstrual bleeding and intermenstrual bleeding were assessed as binary variables (present/absent) based on clinical history and FIGO PALM-COEIN criteria, rather than VAS scoring, given their volumetric rather than pain-based nature. All symptom assessments were performed independently of and prior to review of ultrasound findings, and the assessing investigator was blinded to the anticipated surgical indication and postoperative histopathological outcome. Symptom definitions followed current international guidelines: dysmenorrhea, dyspareunia, dyschezia, and chronic pelvic pain were defined according to the American Society for Reproductive Medicine (ASRM) and European Society of Human Reproduction and Embryology (ESHRE) endometriosis management guidelines [13,14]. Heavy menstrual bleeding (HMB) and intermenstrual bleeding (IB) were defined according to the FIGO PALM–COEIN classification system for abnormal uterine bleeding [9,15].

"Operational definitions applied in this study were as follows

Dysmenorrhea: cyclic pelvic pain occurring during menstruation of sufficient severity to interfere with daily activities, requiring analgesic use or resulting in activity limitation, consistent with ESHRE endometriosis guideline definitions [12].

Dyspareunia: pelvic or genital pain occurring during or after sexual intercourse, assessed as superficial or deep in location, consistent with ASRM and ESHRE definitions [12, 13].

Dyschezia: pain or significant discomfort during defecation, particularly if cyclically exacerbated during the menstrual period, consistent with ESHRE deep endometriosis symptom [12] criteria [12].

Dysuria: pain, burning, or discomfort during urination, recorded irrespective of menstrual cycle phase; urinary tract infection was excluded clinically prior to symptom attribution [12].

Heavy menstrual bleeding (HMB): menstrual blood loss exceeding 80 ml per cycle, or clinically significant menstrual bleeding that impairs physical, social, emotional, or material quality of life, irrespective of measured volume, consistent with FIGO PALM–COEIN criteria [9,14].

Intermenstrual bleeding (IB): uterine bleeding occurring outside the expected menstrual period, including both random and predictable patterns of non-menstrual bleeding, consistent with FIGO PALM–COEIN criteria [9,14].

Chronic pelvic pain (CPP): non-menstrual or non-cyclical pelvic pain persisting for a minimum of six months, located in the anatomical pelvis, anterior abdominal wall, lower back, or buttocks, of sufficient severity to cause functional disability or require medical treatment, consistent with ASRM and ESHRE definitions [12,15].

Abdominal bloating: self-reported sensation of abdominal distension or fullness, recorded as a binary variable (present/absent) based on patient report during structured interview; no validated scoring instrument was applied for this symptom.

Ultrasonographic assessment

All transvaginal ultrasound examinations were performed by two investigators (E.Ç. and M.N.T.), each with a minimum of five years of dedicated experience in gynecological ultrasound and formal training in MUSA-based uterine assessment. Sonographic findings were recorded by consensus following simultaneous dual-operator review of each examination. In cases of disagreement between the two primary investigators, a third senior investigator (Ç.Ç.) with subspecialty expertise in gynecological imaging was consulted for final adjudication. Formal interobserver agreement statistics were not calculated, as all examinations were performed and interpreted by consensus rather than independently; this represents a limitation of the present study. All transvaginal ultrasound examinations were performed using a Mindray DC-80 ultrasound system (Mindray Medical International, Shenzhen, China) equipped with a 3–11 MHz transvaginal transducer. Examinations were conducted with the woman in the dorsal lithotomy position following complete bladder emptying. The uterus was systematically evaluated in both sagittal and transverse planes, with additional oblique plane imaging performed when required for complete myometrial assessment. Uterine length was measured in the sagittal plane from the uterine fundus to the external cervical os. Anterior and posterior myometrial wall thickness was measured from the endometrial-myometrial interface to the serosal surface at the point of maximum thickness in the sagittal plane at the uterine midpoint. All color and power Doppler assessments were performed using standardized gain settings, pulse repetition frequency, and wall filter parameters to minimize operator-dependent variability, consistent with ISUOG technical recommendations. Sonographic evaluation followed the 2022 revised MUSA criteria [8] and included systematic assessment of the following parameters:

- Uterine size: For uterine size analysis, women with sonographically confirmed leiomyomas were excluded to minimize confounding from leiomyoma-related uterine enlargement.
- Myometrial echogenicity: classified as homogeneous or heterogeneous based on the overall myometrial echotexture pattern, excluding areas occupied by discrete lesions.
- Myometrial asymmetry: defined as an absolute difference of more than 5 mm between the anterior and posterior myometrial wall thickness, measured from the endometrial-myometrial interface to the serosal surface in the sagittal plane at the uterine midpoint, consistent with MUSA 2022 consensus definitions [9]. An anterior-to-posterior wall thickness ratio was additionally calculated for descriptive purposes; however, the absolute difference threshold of >5 mm was used as the primary binary criterion for statistical analysis, as ratio-based definitions have demonstrated lower interobserver reproducibility in published MUSA validation studies [8,9,14].
- For assessment of uterine size, myometrial asymmetry, and myometrial heterogeneity, women with sonographically confirmed leiomyomas were excluded from the analysis, as leiomyomas may enlarge the uterus and distort myometrial wall thickness and echogenicity. Accordingly, these parameters were evaluated in a leiomyoma-free subset of the study population (adenomyosis group n=24, control group n=41; total n=65).
- Leiomyomas: the presence, number, FIGO subtype classification, and maximum diameter of leiomyomas were systematically recorded. In analyses of adenomyosis-specific lesion characteristics including lesion echogenicity, shadowing pattern, and vascularization cases with concurrent leiomyomas were analyzed separately and results interpreted with caution, given the potential for leiomyomas to confound myometrial sonographic features.
- Lesion definition: myometrial lesions were categorized as well-defined (typically consistent with leiomyoma, characterized by a distinct echogenic pseudocapsule and smooth borders) or ill-defined (suggestive of adenomyosis, characterized by indistinct margins and gradual transition to surrounding myometrium), consistent with MUSA 2022 criteria [8]. For well-defined lesions, FIGO subtype location, number, and largest diameter were recorded. For ill-defined lesions, distribution pattern (focal or diffuse), estimated depth of myometrial penetration (inner, middle, or outer third), and border characteristics were systematically documented.
- Lesion echogenicity: myometrial lesion echogenicity was classified using the five-tier MUSA grading system as very hypoechoic (−−), hypoechoic (−), isoechoic, hyperechoic (+), or very hyperechoic (++), with the myometrium serving as the reference tissue for echogenicity comparison.
- Myometrial shadowing: the presence, pattern, and intensity of myometrial acoustic shadowing were systematically documented. Shadowing pattern was

classified as: peripheral (edge shadowing, typically associated with leiomyoma), internal (arising from within the lesion), or fan-shaped (arising from the endometrial-myometrial interface and spreading into the myometrium in a fan-like distribution, considered an indirect MUSA marker of adenomyosis). Shadowing intensity was graded as mild, moderate, or strong, consistent with MUSA 2022 definitions [8].

- Myometrial cysts: the presence, sonographic type, number, and largest diameter of myometrial cysts were systematically recorded. Cyst echogenicity was classified according to MUSA 2022 criteria as: anechoic, low-level echoes, ground-glass appearance, or mixed echogenicity [8].The presence of an echogenic rim considered a specific sonographic feature of adenomyosis-related hemorrhagic cysts was specifically documented. Cyst number was recorded as the primary diagnostic parameter, consistent with MUSA guideline recommendations prioritizing cyst count over maximum dimension as the diagnostically relevant metric.

- Hyperechoic islands: the presence, number, and maximum diameter of hyperechoic myometrial islands were recorded. Hyperechoic islands were defined as discrete, well-circumscribed, hyperechoic foci within the myometrium, not associated with acoustic shadowing, and distinct from calcifications, consistent with MUSA 2022 revised definitions [8]. Their presence was recorded as a binary variable (present/absent) for primary statistical analysis.

- Subendometrial echogenic lines and buds: the presence, number, and uterine wall location (anterior, posterior, or both) of subendometrial echogenic lines and buds were systematically recorded. These features were defined as thin, echogenic linear projections or small bud-like echogenic foci arising from the endometrial-myometrial interface and extending into the inner myometrium, representing sonographic correlates of basalis endometrial invagination, consistent with MUSA 2022 revised definitions [8]. Their presence was recorded as a binary variable (present/absent) for primary univariate analysis, with anterior and posterior wall localization assessed separately as secondary endpoints.

- Junctional zone (JZ): the sonographic appearance of the junctional zone was systematically assessed and classified into three categories consistent with MUSA 2022 revised definitions [9]: (i) regular a clearly visible, uniform hypoechoic inner myometrial layer with smooth and well-defined borders; (ii) irregular a visible but non-uniform hypoechoic inner myometrial layer demonstrating focal indentations, interruptions, or asymmetric thickening without complete loss of continuity; and (iii) interrupted a junctional zone that is partially or completely disrupted, with loss of the continuous hypoechoic layer and direct interface between endometrium and outer myometrium. For primary statistical analysis, junctional zone status was dichotomized as regular versus irregular or interrupted, consistent with MUSA 2022 consensus recommendations [9]. Three-dimensional ultrasound was not available in this study; JZ assessment was therefore performed exclusively in two-dimensional sagittal and transverse planes, which may have limited detection sensitivity compared to 3D coronal plane reconstruction as reported in published comparative studies [8].

- Vascularization: myometrial lesion vascularization was assessed using color and power Doppler imaging and categorized according to MUSA 2022 definitions [8] as: (i) absent no detectable vascular signal within or around the lesion; (ii) intralesional — vascular signals distributed randomly within the lesion without a specific pattern; (iii) translesional — vascular signals traversing the lesion in a linear or branching pattern from periphery to center; and (iv) circumferential — vascular signals forming a peripheral rim around the lesion. Doppler parameters including gain, pulse repetition frequency, and wall filter settings were standardized across all examinations to minimize operator-dependent variability, consistent with ISUOG technical recommendations.

Grouping

Preoperative symptoms and ultrasound data were recorded independently. Final grouping was based on postoperative histopathology: patients with histopathologically confirmed adenomyosis comprised Group 1 (n = 52) and those without adenomyosis comprised Group 2 (control, n = 125).

Statistical analysis

Data are summarized using descriptive statistics. Continuous variables are presented as mean ± Standard Deviation (SD) for normally distributed data, or as median with minimum–maximum range for non-normally distributed data; categorical variables are presented as absolute frequency and percentage [n (%)]. Normality of continuous variables was assessed using the Kolmogorov–Smirnov test with Lilliefors correction; variables with a test statistic yielding $p<0.05$ were treated as non-normally distributed. For comparisons between two independent groups, Student's independent samples t-test was used for normally distributed continuous variables and the Mann–Whitney U test was used for non-normally distributed continuous variables. Categorical variables were compared between groups using the Pearson chi-square test; Fisher's exact test was applied where any expected cell count was less than five. A two-sided p-value of less than 0.05 was considered statistically significant for all analyses. All statistical analyses were performed using IBM SPSS Statistics version 26.0 (IBM Corp., Armonk, NY, USA).

Associations between individual clinical and sonographic variables and histopathologically confirmed adenomyosis were evaluated by univariate binary logistic regression analysis, with adenomyosis status (present/absent) as the binary dependent variable. Odds Ratios (ORs) with 95% Confidence Intervals (CIs) and corresponding two-sided p-values are reported for each variable. Continuous variables were entered into logistic regression as continuous predictors; categorical variables were entered as binary or nominal dummy-coded predictors as appropriate. Multivariable logistic regression was not performed owing to the exploratory nature of the study, the relatively small number of outcome events (n=52 adenomyosis cases), and the associated risk of model overfitting with multiple candidate predictors; the rule of thumb of a minimum of ten outcome events per predictor variable was used as the guiding criterion. Variables demonstrating p<0.10 in univariate analysis were recorded as candidates for inclusion in future multivariable modeling in larger independent cohorts.

Diagnostic performance metrics including sensitivity, specificity, positive predictive value (PPV), and Negative Predictive Value (NPV) were calculated for each statistically significant MUSA criterion and for each statistically significant clinical symptom variable, using histopathologically confirmed adenomyosis as the reference standard. For binary sonographic and clinical variables, a two-by-two contingency table was constructed and diagnostic metrics derived accordingly. Exact binomial 95% confidence intervals were calculated for sensitivity and specificity estimates. Receiver Operating Characteristic (ROC) curve analysis was performed for the composite MUSA score as a continuous ordinal variable; the Area Under the Curve (AUC) with 95% CI was reported as a measure of overall discriminatory performance, where AUC values of 0.50, 0.60–0.70, 0.70–0.80, 0.80–0.90, and >0.90 were interpreted as no discrimination, poor, acceptable, excellent, and outstanding discrimination, respectively. The optimal cut-off threshold for the composite MUSA score was determined using the Youden index (J = sensitivity + specificity – 1), which identifies the threshold maximizing the sum of sensitivity and specificity. Likelihood ratios — positive likelihood ratio (LR+) and negative likelihood ratio (LR–) were additionally calculated for the composite MUSA score at the optimal cut-off to facilitate clinical interpretation of the diagnostic findings."

To evaluate the additive diagnostic value of simultaneously assessed multiple MUSA sonographic criteria, a composite MUSA score was prospectively calculated for each woman by summing eight pre-specified binary MUSA variables: (i) myometrial cysts (present=1, absent=0); (ii) subendometrial echogenic lines and buds (present=1, absent=0); (iii) hyperechoic islands (present=1, absent=0); (iv) myometrial asymmetry (present=1, absent=0); (v) myometrial heterogeneity (present=1, absent=0); (vi) junctional zone status (irregular or interrupted=1, regular=0); (vii) fan-shaped shadowing (present=1, absent=0); and (viii) translesional vascularization (present=1, absent=0); yielding a total composite MUSA score ranging from 0 to 8. These eight variables were selected a priori based on their representation of both direct and indirect MUSA adenomyosis markers as defined in the 2022 revised MUSA consensus [9] and were not selected post-hoc based on univariate analysis results, to avoid incorporation bias.

Junctional zone status was dichotomized as regular versus irregular or interrupted per MUSA 2022 definitions [9]. The composite score was compared between groups using the Mann–Whitney U test and evaluated by ROC analysis; AUC, optimal cut-off via Youden index, sensitivity, specificity, PPV, and NPV are reported. Women were stratified as low risk (0–1), intermediate risk (2–3), or high risk (≥4); adenomyosis distribution across categories was assessed by chi-square test for trend.

Results

Demographic characteristics and symptom scores of patients with and without adenomyosis are summarized in **Table 1**. Mean age was similar between groups (46.4 ± 4.1 vs 46.4 ± 3.8 years; p>0.9; OR=0.99, 95% CI: 0.92–1.07). Gravidity was comparable (median 3 [1–6] vs 3 [1–7]; p>0.9; OR=1.21, 95% CI: 0.96–1.54). Parity did not differ significantly between groups (median 3 [1–5] vs 2 [1–5]; p>0.9; OR=1.01, 95% CI: 0.76–1.37). Number of living children was also similar (median 3 [1–5] vs 2 [1–5]; p=0.60; OR=1.07, 95% CI: 0.71–1.60).

Regarding symptom scores, dysmenorrhea was higher in the adenomyosis group but the difference was not statistically significant (median 4 [0–10] vs 2 [0–10]; p=0.21; OR=1.06, 95% CI: 0.96–1.16). Dyspareunia showed a significant positive association with adenomyosis (median 2 [0–10] vs 0 [0–10]; p = 0.02; OR = 1.11, 95% CI: 1.01–1.23). No difference was observed for dyschezia (median 0 [0–10] vs 0 [0–10]; p=0.88; OR=1.02, 95% CI: 0.91–1.16) or dysuria (median 0 [0–7] vs 0 [0–10]; p=0.36; OR=0.95, 95% CI: 0.81–1.11).

Heavy menstrual bleeding was significantly more frequent in the adenomyosis group (75.0% vs 38.4%; p<0.001; OR=4.81, 95% CI: 2.33–9.92), representing the strongest clinical predictor of adenomyosis in this cohort. Intermenstrual bleeding (IB) did not differ between groups (9.6% vs 13.6%; p=0.46; OR=0.68, 95% CI: 0.24–1.94). Bloating was more common in the adenomyosis group but not statistically significant (63.5% vs 52%; p=0.16; OR=1.60, 95% CI: 0.83–3.12). Chronic pelvic pain was observed more frequently in the adenomyosis group (42.3% vs 34.4%) but this difference was not significant (p=0.32; OR=1.39, 95% CI: 0.72–2.71).

Table 1. Demographic characteristics and symptom scores by group.

Variables		Adenomyosis (n=52)	No adenomyosis (n=125)	P value	OR (95% CI)
Age (years)		46.4 (±4.1)	46.4 (±3.8)	>0.9	0.99 (0.92–1.07)
Gravidity		3 (1-6)	3 (1-7)	>0.9	1.21 (0.96–1.54)
Parity		3 (1–5)	2 (1–5)	>0.9	1.01 (0.76–1.37)
Living children		3 (1–5)	2 (1–5)	0.60	1.07 (0.71–1.60)
Dysmenorrhea		4 (0–10)	2 (0–10)	0.21	1.06 (0.96–1.16)
Dyspareunia		2 (0–10)	0 (0–10)	**0.02**	1.11 (1.01–1.23)
Dyschezia		0 (0–10)	0 (0–10)	0.88	1.02 (0.91–1.16)
Dysuria		0 (0–7)	0 (0–10)	0.36	0.95 (0.81–1.11)
HMB	Yes	39 (75)	48 (38.4)	**<0.001**	4.81 (2.33–9.92)
	No	13 (25)	77 (61.6)		
IB	Yes	5 (9.6)	17 (13.6)	0.46	0.68 (0.24–1.94)
	No	47 (90.4)	108 (86.4)		
Bloating	Yes	33 (63.5)	65 (52)	0.16	1.60 (0.83–3.12)
	No	19 (36.5)	60 (48)		
CPP	Yes	22 (42.3)	43 (34.4)	0.32	1.39 (0.72–2.71)
	No	30 (57.7)	82 (65.6)		

HMB: Heavy Menstrual Bleeding; IB: Intermenstrual Bleeding; CPP: Chronic Pelvic Pain; OR: Odds Ratio; 95% CI: 95% Confidence Interval. Data are presented as mean ± standard deviation, median (min–max), or n (%) as appropriate. p<0.05 was considered statistically significant.

Heavy Menstrual Bleeding (HMB) showed the highest sensitivity at 75% with a specificity of 61.6%. Intermenstrual Bleeding (IB) had very low sensitivity (9.6%) but high specificity (86.4%). Bloating demonstrated moderate sensitivity (63.5%) with low specificity (48.0%), while Chronic Pelvic Pain (CPP) was associated with lower sensitivity (42.3%) and moderate specificity (65.6%). Overall, HMB emerged as the most sensitive clinical symptom, whereas IB provided the greatest specificity for adenomyosis. Cyst size, number of islands, presence of echogenic line and myometrial features between patients with and without adenomyosis. In the leiomyoma-free subset, mean uterine length was 90.7±9.4 mm in the adenomyosis group and 87.4±16.9 mm in the control group.

Myometrial cysts were significantly more frequent in the adenomyosis group (67.3%, 35/52) than in the control group (38.4%, 48/125) ($p < 0.001$; OR = 3.30, 95% CI: 1.67–6.56). Cyst number was higher in the adenomyosis group (median 3 [1–6] vs 2 [1–7]) and this difference was statistically significant ($p = 0.02$; OR = 1.37, 95% CI: 0.98–1.98). Although the median maximum echogenic cyst size was 7 mm (2–15) in the adenomyosis group and 8 mm (1.3–49) in the control group, this difference was not significant ($p = 0.12$; OR = 0.90, 95% CI: 0.81–1.00). Hyperechoic islands were observed in 15.4% (8/52) of the adenomyosis group and 6.4% (8/125) of controls; this difference approached but did not reach statistical significance ($p = 0.058$; OR = 2.67, 95% CI: 0.94–7.52). The number of islands (median 2 [1–5] vs 1.5 [1–3]) and the maximum island size (median 11 mm in both groups) did not differ significantly ($p = 0.43$ and $p > 0.9$, respectively).

Myometrial asymmetry was assessable in a subset of women without concurrent leiomyomas distorting uterine architecture (adenomyosis group n=24, control group n=41). In this leiomyoma-free subset, myometrial asymmetry was significantly more common in the adenomyosis group (62.5% vs 19.5%; p<0.001; OR=6.88, 95% CI: 2.22–21.3). Similarly, myometrial heterogeneity was significantly more frequent in the adenomyosis group within this subset (87.5% vs 58.5%; p=0.015; OR=4.96, 95% CI: 1.28–19.3). These analyses were restricted to leiomyoma-free cases to avoid confounding of indirect myometrial markers by concurrent leiomyoma-related architectural distortion. Subendometrial echogenic lines and buds were detected in 17.3% (9/52) of the adenomyosis group versus 2.4% (3/125) of controls, representing the highest specificity MUSA criterion identified in this study (specificity 97.6%, PPV 75.0%). Anterior and posterior positive subendometrial findings were more frequent in the adenomyosis group (anterior 3.8% vs 0.8%; posterior 13.5% vs 1.6%), with posterior localization showing a significant association (OR = 9.93, 95% CI: 1.98–49.6).

Table 2. Ultrasonographic data by group: Key measurements (uterine length, cyst and island features).

Variables		Adenomyosis (n=52)	No adenomyosis (n=125)	P value	OR (95% CI)
Uterine length (mm)		90.7 (±9.4)	87.4 (±16.9)	0.59	0.99 (0.99–1.01)
Myometrial cysts	Yes	35 (67.3)	48 (38.4)	**<0.001**	**3.30 (1.67–6.56)**
	No	17 (32.7)	77 (61.6)		
	Number	3 (1–6)	2 (1–7)	**0.02**	**1.37 (0.98–1.98)**
	Max echogenic cyst size (mm)	7 (2–15)	8 (1.3–49)	0.12	0.90 (0.81–1.00)
Hyperechoic islands	Yes	8 (15.4)	8 (6.4)	0.058	2.67 (0.94–7.52)
	No	44 (84.6)	117 (93.6)		
	Numbers	2 (1–5)	1.5 (1–3)	0.43	1.63 (0.57–4.65)
	Max island size (mm)	11 (0.7–17)	11 (3.2–20)	>0.9	0.97 (0.81–1.17)
Myometrial asymmetry	Yes	15 (62.5)	8 (19.5)	**<0,001**	6.88 (2.22–21.3)
	No	9 (37.5)	33 (80.5)		
Myometrial heterogeneity	Yes	21(87.5)	24 (58.5)	**0.015**	4.96 (1.28–19.3)
	No	3 (12.5)	17 (41.5)		
Subendometrial echogenic line and buds	Positive	9 (17.6)	3 (2.4)	**<0.001**	8.51 (2.20–32.9)
	Negative	122 (97.6)	43 (82.7)		
	Numbers	3 (1–6)	2 (1–7)	0.73	1.60 (0.24–10.9)
	Negative	43 (82.7)	122 (97.6)	**<0.001**	-
	Positive (+/anterıor)	2 (3.8)	1 (0.8)		5.58 (0.50–64.2)
	Positive (+/posterıor)	7 (13.5)	2 (1.6)		9.93 (1.98–49.6)

Myometrial cysts showed a sensitivity of 67.3% and a specificity of 61.6%. Hyperechoic islands had low sensitivity (15.4%) but high specificity (93.6%). Myometrial asymmetry demonstrated a sensitivity of 62.5% and a specificity of 80.5%. Myometrial heterogeneity was highly sensitive (87.5%) but less specific (41.5%). Subendometrial echogenic line and buds presented a sensitivity of 17.3% with very high specificity (97.6%). Overall, myometrial heterogeneity emerged as the most sensitive finding, while subendometrial echogenic line and buds provided the greatest specificity for adenomyosis.

Table 3 summarizes the comparison of well-defined versus ill-defined lesions, myometrial lesion echogenicity, junctional zone appearance, and vascularization patterns between patients with and without adenomyosis. Well-defined lesions (typically compatible with leiomyoma/myoma) were observed in 57.7% (30/52) of the adenomyosis group and 67.2% (84/125) of the control group, with no significant difference (p = 0.22; OR = 0.66, 95% CI: 0.34–1.30). Ill-defined lesions were mostly absent (adenomyosis 86.5% vs control 90.4%); there were no significant differences for focal type (5.8% vs 6.4%; OR = 0.94, 95% CI: 0.24–3.71) or diffuse type (7.7% vs 3.2%; OR = 2.51, 95% CI: 0.60–10.5) (p = 0.42).

Myometrial lesion echogenicity did not differ significantly between groups for isoechoic (38.5% vs 34.4%), hypoechoic (13.5% vs 11.2%; OR = 0.88, 95% CI: 0.41–1.90), hyperechoic (9.6% vs 20.8%; OR = 0.95, 95% CI: 0.33–2.80), or very hypoechoic lesions (1.9% vs 1.6%; OR = 0.95, 95% CI: 0.08–11.1) (p = 0.37). Conversely, very hyperechoic lesions were absent in the adenomyosis group and present in 3.2% (4/125) of controls; owing to zero cells in the adenomyosis group, a meaningful odds ratio could not be estimated by standard logistic regression (complete separation); this finding is reported descriptively only.

Junctional zone assessment in the adenomyosis group showed regular 40.4% (21/52), irregular 38.5% (20/52), and interrupted 21.2% (11/52). In controls, the distribution was regular 55.2% (69/125), irregular 20.8% (26/125), and interrupted 24.0% (30/125).

Shadowing patterns in the adenomyosis group were fan-shaped 28.8% (n = 15), internal 21.2% (n = 11), and peripheral 13.3% (n = 7); in the non-adenomyosis group these were 33.6% (n = 42), 25.6% (n = 32), and 11.2% (n = 14), respectively. Among cases without shadowing, adenomyosis was present in 36.5% (n = 19) versus 29.6% (n = 37) in the control group. These differences were not statistically significant (p = 0.73).

Table 3. Ultrasonographic characteristics of myometrial lesions, junctional zone, shadowing, and vascularization in patients with and without adenomyosis.

Variables			Adenomyosis (n=52)	No adenomyosis (n=125)	P value	OR (95% CI)
Myometrial lesion	Well-defined (leiomyoma	**Negative**	22 (42.3)	41 (38.8)	0.22	0.66 (0.34–1.30)
		Positive	30 (57.70)	84 (67.20)		
	Ill-defined lesion	**Negative**	45 (86.5)	113 (90.4)	0.42	-
		Positive (focal)	3 (5.8)	8 (6.4)		0.94 (0.24–3.71)
		Positive (diffuse)	4 (7.7)	4 (3.2)		2.51 (0.60–10.5)
Myometrial lesion	Isoechoic		20 (38.5)	43 (34.4)	0.37	-
echogenicity	Hypoechoic		7 (13.5)	14 (11.2)		0.88 (0.41–1.9)
	Hyperechoic		5 (9.6)	26 (20.8)		0.95 (0.33–2.8)
	Very hypoechoic		1 (1.9)	2 (1.6)		0.95 (0.08–11.1)
	Very hyperechoic		0	4 (3.2)		Not estimable
Junction Zone	Regular		21 (40.4)	69 (55.2)	**0.047**	**-**
	Irregular		20 (38.5)	26 (20.8)		2.57 (1.18–5.40)
	Interrupted		11 (21.2)	30 (24)		1.21 (0.52–2.81)
	Regular		21 (40.4)	69 (55.2)	0.073	1.81 (0.94–3.50)
	Irregular and Interrupted		31 (59.6	56 (44.8)		
Shadowing	No		19 (36.5)	37 (29.6)	0.73	-
	Fan-shape shadowing		15 (28.8)	42 (33.6)		0.69 (0.31–1.56)
	Internal Shadowing		11 (21.2)	32 (25.6)		0.67 (0.29–1.61)
	Edge Shadowing		7 (13.5)	14 (11.2)		0.97 (0.34–2.80)
Vascularization of	Absent		20 (38.5)	38 (30.4)	0.22	-
Myometrial lesion	Intralesional		12 (23.1)	37 (29.6)		0.62 (0.26–1.44)
	Translesional		5 (9.6)	24 (19.2)		0.39 (0.13–1.19)
	Circumferential		15 (28.8)	26 (20.8)		1.09 (0.48–2.53)

OR: Odds Ratio; 95% CI: 95% Confidence Interval. Data are presented as mean ± standard deviation, median (min– max), or n (%) as appropriate. p <0.05 was considered statistically significant.

No significant differences were found in lesion vascularization between groups. Absence of vascularization was observed in 38.5% (20/52) of the adenomyosis group and 30.4% (38/125) of controls (p = 0.22). Intralesional vascularization was present in 23.1% (12/52) of adenomyosis cases and 29.6% (37/125) of controls (OR = 0.62, 95% CI: 0.26–1.44). Translesional vascularization was observed in 9.6% (5/52) of the adenomyosis group and 19.2% (24/125) of controls, without statistically significant difference (OR=0.39, 95% CI: 0.13–1.19; p=0.10). Circumferential vascularization was observed in 28.8% (15/52) of adenomyosis patients and 20.8% (26/125) of controls (OR = 1.09, 95% CI: 0.48–2.53).

Table 4 summarizes the distribution of MUSA scores between patients with and without adenomyosis, presenting median values and risk group classifications along with their statistical significance. The composite MUSA score was significantly higher in the adenomyosis group than in the control group (median 3.0, range 0–5 versus median 2.0, range 0–5; Mann–Whitney U test, p=0.003), confirming the additive diagnostic value of simultaneously assessed multiple MUSA criteria.

Risk stratification demonstrated a significant difference in adenomyosis prevalence across MUSA score categories (chi-square test for trend, p=0.002): adenomyosis was confirmed in 20.0% (7/35) of low-risk women (score 0–1), 24.5% (26/106) of intermediate-risk women (score 2–3), and 52.8% (19/36) of high-risk women (score ≥4), representing a significant stepwise increase in adenomyosis probability with increasing composite score. Conversely, the majority of non-adenomyosis patients fell into the intermediate risk category (64.0%), while 50.0% of adenomyosis patients were also in this group. The chi-square test confirmed a statistically significant association between MUSA risk categories and adenomyosis status (p = 0.002).

Table 4. Comparison of MUSA score between adenomyosis and non-adenomyosis groups.

Variables		Adenomyosis (n=52)	No adenomyosis (n=125)	P value
MUSA score points		3.0 (0–5)	2.0 (0–5)	0.003
MUSA Score	Low risk	7 (13.5%)	28 (22.4%)	0.002
	Intermediate risk	26 (50.0%)	80 (64.0%)	
	High risk	19 (36.5%)	17 (13.6%)	

MUSA = Morphological Uterus Sonographic Assessment, OR = Odds Ratio, CI = Confidence Interval, SD = Standard Deviation, n = number of cases, p-value = probability value.

ROC curve analysis of the composite MUSA score demonstrated an AUC of 0.636 (95% CI: 0.543–0.729; SE=0.047; p=0.004), indicating poor discriminatory ability per the prespecified AUC classification, though significantly above chance level. At the optimal cut-off of 3.5 (corresponding to a score of ≥4) determined by the Youden index, the composite score yielded a sensitivity of 36.5%, specificity of 86.4%, PPV of 57.6%, and NPV of 75.0%. The high specificity at this threshold indicates that a composite MUSA score of ≥4 functions primarily as a rule-in marker for adenomyosis, whereas the low sensitivity indicates limited ability to exclude adenomyosis when the score is below this threshold.

Table 5. ROC curve analysis of the composite MUSA score for detection of histopathologically confirmed adenomyosis.

Test Variable	AUC (95% CI)	SE	P-value	Optimal Cut-off	Sensitivity (%)	Specificity (%)	PPV (%)	NPV (%)	Youden Index
Musa score	0.636 (0.543–0.729)	0.047	0.004	3.5 (≥4)	36.5	86.4	57.6	75.0	0.229

AUC: Area Under the Curve; CI: Confidence Interval; SE: Standard Error; PPV: Positive Predictive Value; NPV: Negative Predictive Value. The optimal cut-off of 3.5 corresponds to a composite MUSA score of ≥4. Sensitivity, specificity, PPV, NPV, and Youden index were calculated using histopathologically confirmed adenomyosis as the reference standard.

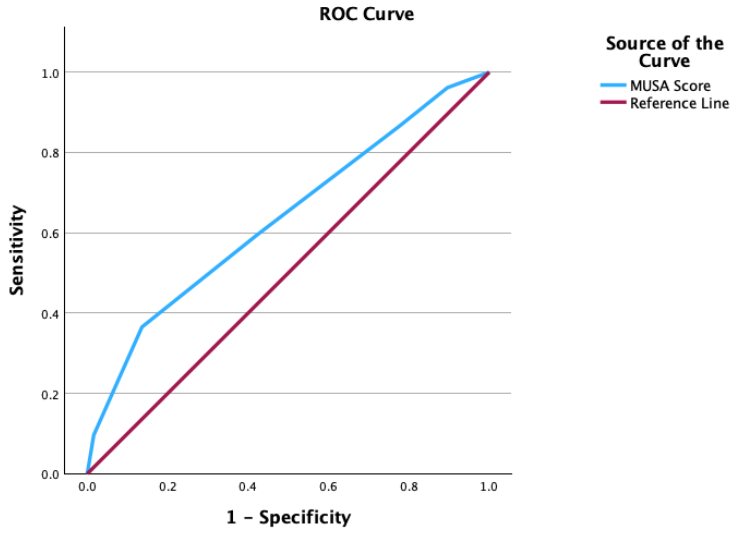

Figure 1. Receiver Operating Characteristic (ROC) curve for the composite MUSA score in the detection of histopathologically confirmed adenomyosis. The blue line represents the discriminatory performance of the composite score; the red diagonal reference line represents chance-level performance (AUC=0.50). The AUC of 0.636 (95% CI: 0.543–0.729; p=0.004) indicates poor discriminatory ability per the prespecified classification, though significantly above chance level. The optimal cut-off of 3.5 (corresponding to a composite MUSA score of ≥4), determined by the Youden index, yielded a sensitivity of 36.5%, specificity of 86.4%, PPV of 57.6%, and NPV of 75.0%. At this threshold, a composite score of ≥4 functions as a rule-in marker for adenomyosis (high specificity, SpPin), whereas a score below this threshold does not reliably exclude the diagnosis.

Discussion

The present study evaluated the diagnostic value of preoperative TVUS using MUSA criteria in 177 women undergoing hysterectomy, with histopathological confirmation serving as the reference standard. Adenomyosis was confirmed in 52 women (29.4%), consistent with previously reported prevalence rates of 20–35% in hysterectomy specimens. The key findings of this study were: (a) heavy menstrual bleeding and dyspareunia were the strongest clinical correlates of adenomyosis; (b) subendometrial echogenic lines/buds, myometrial asymmetry, heterogeneity, cysts, and junctional zone irregularity were the most diagnostically informative MUSA criteria; and (c) uterine size in the leiomyoma-free subset, shadowing patterns, vascularization, and lesion echogenicity demonstrated no significant associations with adenomyosis [9,14]. These findings broadly support the MUSA consensus recommendation for comprehensive multi-criterion evaluation rather than reliance on any single sonographic feature.

No significant differences in age, gravidity, parity, or number of living children were observed between groups, consistent with contemporary evidence challenging the classical characterization of adenomyosis as a disease exclusively of older multiparous women. The mean age of approximately 46 years in both groups reflects the hysterectomy population rather than the broader adenomyosis population; advanced imaging now enables diagnosis in younger and nulliparous women who would not historically have been captured in hysterectomy-based prevalence studies [7,12,16,17]. These findings support the view that demographic factors alone are insufficient to guide clinical suspicion for adenomyosis and that objective imaging-based assessment is essential across all age and parity groups.

Adenomyosis is most often associated with heavy menstrual bleeding, dysmenorrhea, chronic pelvic pain, and infertility [6,17]. However, these symptoms are not specific, as similar complaints occur in leiomyoma, endometriosis, and other benign gynecological conditions. Therefore, diagnosis cannot rely solely on clinical findings. Heavy menstrual bleeding was the strongest clinical predictor of adenomyosis in our cohort, increasing the likelihood of histopathologically confirmed disease nearly fivefold. This finding is consistent with previous evidence identifying heavy menstrual bleeding as a frequent manifestation of adenomyosis and may be explained by impaired uterine contractility and hemostasis, local inflammation, aberrant angiogenesis, progesterone resistance, and increased endometrial surface area secondary to myometrial hypertrophy [17,19,20]. Accordingly, adenomyosis should be considered in the differential diagnosis of women presenting with unexplained or treatment-resistant heavy menstrual bleeding.

Dyspareunia was significantly associated with adenomyosis in our cohort (p=0.02; OR=1.11), albeit with a modest effect size. This association is likely mediated by posterior myometrial wall involvement, which has been demonstrated in up to 60% of adenomyosis cases. The proposed mechanisms include increased density of substance P-positive nerve fibers within adenomyotic lesions, elevated expression of pro-inflammatory cytokines including IL-1β, IL-6, and TNF-α, enhanced local prostaglandin E2 synthesis, and sensitization of pelvic nociceptors through repeated inflammatory stimulation [15,17,18]. Notably, the co-occurrence of deep infiltrating endometriosis — which shares overlapping symptom profiles and is present in 35–80% of adenomyosis cases — may have contributed to dyspareunia scores in our cohort, as endometriosis was not systematically excluded. Future studies should prospectively stratify dyspareunia analysis by endometriosis status to better isolate the adenomyosis-specific contribution.

Contrary to the classical association between adenomyosis and dysmenorrhea, our study found no statistically significant difference in dysmenorrhea VAS scores between groups (p=0.21; OR=1.06). This finding warrants careful interpretation for several reasons. First, dysmenorrhea is inherently non-specific, occurring in leiomyoma, endometriosis, primary dysmenorrhea, and pelvic inflammatory disease all of which were present in our surgical cohort. Second, the use of VAS as a continuous measure rather than a binary present/absent variable may have reduced statistical power to detect group differences. Third, preoperative analgesic or hormonal medication use — which was not systematically recorded may have attenuated reported pain scores in both groups. Fourth, the relatively advanced mean age of our cohort (46.4 years) may reflect a shift toward HMB as the dominant symptom, as dysmenorrhea severity has been reported to paradoxically decrease with age in some adenomyosis phenotypes. These considerations suggest that the absence of a significant dysmenorrhea association in our study reflects methodological factors rather than a true biological absence of this symptom [3]. Intermenstrual bleeding and bloating also lacked diagnostic value, being reported as nonspecific supportive findings rather than primary indicators [1,16].

Among direct MUSA markers, myometrial cysts were significantly more frequent in the adenomyosis group (67.3% vs 38.4%; OR=3.30; p<0.001). Histopathologically, these cysts represent dilated ectopic endometrial glandular spaces within the myometrium, often related to cyclic hemorrhage and fluid accumulation. Although MUSA 2022 classifies myometrial cysts as a direct marker of adenomyosis, the specificity in our cohort was lower than that reported in dedicated ultrasound studies, probably reflecting the high prevalence of coexisting leiomyomas and other non-adenomyosis-related cystic or pseudocystic myometrial changes. Importantly, cyst number

rather than maximum cyst size was the diagnostically relevant parameter, supporting MUSA recommendations to document cyst count during structured reporting. Hyperechoic islands showed a borderline association with adenomyosis (p=0.058; OR=2.67), suggesting a potential confirmatory role in larger cohorts because of their low sensitivity but relatively high specificity profile [4,17].

Myometrial asymmetry demonstrated one of the strongest associations with adenomyosis in the leiomyoma-free subset of our cohort (OR=6.88, 95% CI: 2.22–21.3; sensitivity 62.5%, specificity 80.5%), consistent with findings of Van den Bosch et al. and the MUSA 2022 Delphi consensus [7,8]. Since leiomyomas can directly distort myometrial wall thickness and confound asymmetry assessment, this analysis was intentionally restricted to leiomyoma-free cases. The relatively modest sensitivity indicates that absence of asymmetry does not reliably exclude adenomyosis, particularly in early or focal disease.

Myometrial heterogeneity demonstrated the highest sensitivity among all MUSA criteria in the leiomyoma-free subset (87.5%), albeit with limited specificity (41.5%), consistent with its role as a sensitive but non-specific indirect adenomyosis marker reflecting disorganized myometrial architecture and fibrotic stromal changes [4]. Given that heterogeneity assessment was restricted to leiomyoma-free cases in the present study, the observed specificity may be higher than would be expected in an unselected hysterectomy population where concurrent leiomyomas frequently produce heterogeneous myometrial echotexture.

No significant differences were observed for well- or ill-defined lesions and fibroid presence. The coexistence of leiomyomas is frequently reported, with hysterectomy series showing rates of 35–60% [3,12]. Fibroids complicate diagnosis due to acoustic shadowing and distortion but are not protective or risk-enhancing factors. Similarly, lesion echogenicity patterns were not distinctive, as described in MUSA-based sonographic assessment studies [14,16].

Neither myometrial shadowing patterns nor vascularization characteristics demonstrated significant associations with adenomyosis in our cohort (p=0.73 and p=0.22, respectively). These negative findings are consistent with published meta-analyses reporting high operator dependency and low interobserver reproducibility for both parameters. Fan-shaped shadowing, while described in the MUSA consensus as an indirect adenomyosis marker, has been shown to have limited standalone diagnostic value when evaluated independently of other criteria, with sensitivity estimates of 30–40% and wide confidence intervals across studies. Similarly, Doppler-based vascularization assessment is highly technique-dependent; standardized gain settings, pulse repetition frequency, and wall filter parameters critically influence vascular signal detection, and the absence of a standardized Doppler protocol in our study may have reduced the reliability of these assessments. MUSA consensus recommendations support interpreting Doppler findings as supportive features within a comprehensive MUSA evaluation rather than as primary diagnostic criteria, a recommendation strongly supported by our finding [16].

Subendometrial echogenic lines and buds demonstrated the strongest sonographic association with adenomyosis in our cohort (OR=8.51, 95% CI: 2.20–32.9; p<0.001) and the highest specificity among evaluated MUSA criteria (97.6%). Despite low sensitivity, their presence can therefore be considered a strong rule-in marker. Posterior wall localization showed a particularly strong association, consistent with the reported predilection of adenomyosis for the posterior myometrium. Histopathologically, these findings likely represent basalis endometrial invaginations into the inner myometrium, supporting the junctional zone invagination hypothesis. Their low sensitivity in this study may partly reflect the exclusive use of two-dimensional TVUS, as three-dimensional coronal plane reconstruction improves assessment of subendometrial and junctional zone abnormalities [8, 9].

Junctional zone irregularity was significantly associated with adenomyosis in our cohort (OR=2.57, 95% CI: 1.18–5.40; p=0.047), with a calculated sensitivity of 48.8% and specificity of 72.6%. The junctional zone, representing the inner myometrium adjacent to the endometrial basalis, is the primary site of adenomyosis initiation according to the invagination hypothesis. Its disruption manifesting sonographically as irregularity or interruption of the hypoechoic inner myometrial layer is considered a pathognomonic early marker of adenomyosis. The relatively modest sensitivity observed in our 2D TVUS study is consistent with published literature demonstrating superior JZ assessment with 3D ultrasound and MRI. Harmsen et al. demonstrated that 3D TVUS achieves substantially higher interobserver agreement for JZ assessment compared to 2D TVUS, and MRI-based JZ thickness exceeding 12 mm has been established as a validated diagnostic threshold. The use of 2D TVUS in our study may therefore have underestimated the true diagnostic value of JZ assessment; future studies incorporating 3D TVUS or MRI are needed to fully characterize JZ performance in this [19].

Several limitations should be considered. First, this was a single-center study, which may limit generalizability. Second, formal interobserver agreement could not be calculated because ultrasound examinations were performed by simultaneous dual-operator consensus review rather than independent assessment; this should be addressed in future studies. Third, although all hysterectomy specimens were reviewed by a single blinded gynecological pathologist using standardized diagnostic criteria and 3–5 mm tissue sampling intervals, histopathological diagnosis of adenomyosis may

still be affected by sampling error because adenomyotic foci can be patchy and heterogeneous. Fourth, the exclusion of women using hormonal therapy within three months before ultrasound may reduce, but cannot completely eliminate, the potential effect of prior or unreported hormonal exposure on myometrial echogenicity or junctional zone appearance. Fifth, the absence of multivariable logistic regression limits assessment of independent predictors after adjustment for confounders. Sixth, endometriosis was not systematically recorded, preventing evaluation of its potential confounding effect on symptoms and sonographic findings.

Conclusion

Our findings support the use of structured preoperative TVUS assessment in women scheduled for hysterectomy. Evaluation should focus on the MUSA criteria most strongly associated with adenomyosis in this cohort: myometrial cysts, myometrial asymmetry, myometrial heterogeneity, subendometrial echogenic lines/buds, and junctional zone irregularity. Multiple positive criteria may increase diagnostic suspicion and support preoperative counseling, particularly in women with heavy menstrual bleeding and dyspareunia. MRI may be considered when TVUS findings are equivocal or technically limited.

Conflict of Interest

The authors declare no conflict of interest.

Funding

This research received no specific grant from any funding agency in the public, commercial, or not-for-profit sectors.

Author Contributions

Merve Nur Taşpınar contributed to data collection, ultrasound assessment, data organization, and manuscript preparation. Çetin Çelik contributed to ultrasound assessment, clinical supervision, interpretation of findings, and critical manuscript revision. Ersin Çintesun contributed to study conception and design, data collection, ultrasound assessment, supervision, and manuscript revision. All authors reviewed and approved the final manuscript.

Acknowledgements

None declared.

References

1. Vannuccini S, Tosti C, Carmona F, Huang SJ, Chapron C, Guo SW, et al. Pathogenesis of adenomyosis: an update on molecular mechanisms. Reprod Biomed Online. 2017 Nov;35(5):592–601.
2. Farquhar C, Brosens I. Medical and surgical management of adenomyosis. Best Pract Res Clin Obstet Gynaecol. 2006 Aug;20(4):603–16.
3. Struble J, Reid S, Bedaiwy MA. Adenomyosis: A Clinical Review of a Challenging Gynecologic Condition. J Minim Invasive Gynecol. 2016 Feb 1;23(2):164–85.
4. Biasioli A, Degano M, Restaino S, Bagolin M, Moro F, Ciccarone F, et al. Innovative Ultrasound Criteria for the Diagnosis of Adenomyosis and Correlation with Symptoms: A Retrospective Re-Evaluation. Biomedicines. 2024 Feb 19;12(2):463.
5. Dueholm M, Lundorf E. Transvaginal ultrasound or MRI for diagnosis of adenomyosis. Curr Opin Obstet Gynecol. 2007 Dec;19(6):505–12.
6. Van den Bosch T, de Bruijn AM, de Leeuw RA, Dueholm M, Exacoustos C, Valentin L, et al. Sonographic classification and reporting system for diagnosing adenomyosis. Ultrasound Obstet Gynecol. 2019 May;53(5):576–82.
7. Van den Bosch T, Dueholm M, Leone FP, Valentin L, Rasmussen CK, Votino A, et al. Terms, definitions and measurements to describe sonographic features of myometrium and uterine masses: a consensus opinion from the Morphological Uterus Sonographic Assessment (MUSA) group. Ultrasound Obstet Gynecol. 2015 Sep;46(3):284–98.
8. Harmsen MJ, Van den Bosch T, de Leeuw RA, Dueholm M, Exacoustos C, Valentin L, et al. Consensus on revised definitions of Morphological Uterus Sonographic Assessment (MUSA) features of adenomyosis: results of modified Delphi procedure. Ultrasound Obstet Gynecol. 2022 Jul;60(1):118–31.
9. Munro MG, Critchley HO, Fraser IS. The FIGO classification of causes of abnormal uterine bleeding: Malcolm G. Munro, Hilary O.D. Crithcley, Ian S. Fraser, for the FIGO Working Group on Menstrual Disorders. Int J Gynaecol Obstet. 2011 Apr;113(1):1–2.
10. Bazot M, Daraï E. Role of transvaginal sonography and magnetic resonance imaging in the diagnosis of uterine adenomyosis. Fertil Steril. 2018 Mar;109(3):389–97.
11. Champaneria R, Abedin P, Daniels J, Balogun M, Khan KS. Ultrasound scan and magnetic resonance imaging for the diagnosis of adenomyosis: systematic review comparing test accuracy. Acta Obstet Gynecol Scand. 2010 Nov;89(11):1374–84.
12. Bird CC, McElin TW, Manalo-Estrella P. The elusive adenomyosis of the uterus--revisited. Am J Obstet Gynecol. 1972 Mar;112(5):583–93.
13. Dunselman GA, Vermeulen N, Becker C, Calhaz-Jorge C, D'Hooghe T, De Bie B, et al. ESHRE guideline: management of women with endometriosis. Hum Reprod. 2014 Mar;29(3):400–12.
14. Practice Committee of the American Society for Reproductive Medicine. Endometriosis and infertility: a committee opinion. Fertil Steril. 2012 Sep;98(3):591–8.
15. Fraser IS, Critchley HO, Munro MG, Broder M; Writing Group for this Menstrual Agreement Process. A process designed to lead to

international agreement on terminologies and definitions used to describe abnormalities of menstrual bleeding. Fertil Steril. 2007 Mar;87(3):466–76.

16. Maignien C, Bourdon M, Parpex G, Ferreux L, Patrat C, Bordonne C, et al. Endometriosis-related infertility: severe pain symptoms do not impact assisted reproductive technology outcomes. Hum Reprod. 2024 Feb 1;39(2):346–54.
17. Munro MG, Critchley HOD, Fraser IS; FIGO Menstrual Disorders Committee. The two FIGO systems for normal and abnormal uterine bleeding symptoms and classification of causes of abnormal uterine bleeding in the reproductive years: 2018 revisions. Int J Gynaecol Obstet. 2018 Dec;143(3):393–408.
18. Martire FG, Costantini E, D'Abate C, Schettini G, Sorrenti G, Centini G, et al. Endometriosis and Adenomyosis: From Pathogenesis to Follow-Up. Curr Issues Mol Biol. 2025 Apr 24;47(5):298.
19. Younes G, Tulandi T. Effects of adenomyosis on in vitro fertilization treatment outcomes: a meta-analysis. Fertil Steril. 2017 Sep;108(3):483–90.e3.
20. Dueholm M. Transvaginal ultrasound for diagnosis of adenomyosis: a review. Best Pract Res Clin Obstet Gynaecol. 2006 Aug;20(4):569–82.
21. As-Sanie S, Ross WT, Till SR. Evaluation and Treatment of Chronic Pelvic Pain. Obstet Gynecol. 2026 Jan 1;147(1):21–43.
22. Zondervan KT, Becker CM, Missmer SA. Endometriosis. N Engl J Med. 2020 Mar 26;382(13):1244–56.
23. Harmsen MJ, Trommelen LM, de Leeuw RA, Tellum T, Juffermans LJM, Griffioen AW, et al. Uterine junctional zone and adenomyosis: comparison of MRI, transvaginal ultrasound and histology. Ultrasound Obstet Gynecol. 2023 Jul;62(1):42–60.